Moving quantum states without SWAP via intermediate higher-dimensional qudits

Amit Saha[1,2,*] Debasri Saha,[1] and Amlan Chakrabarti[1,†]

[1]*A. K. Choudhury School of Information Technology, University of Calcutta, Calcutta 700106, India*
[2]*ATOS, Pune 411045, India*

Quantum algorithms can be realized in the form of a quantum circuit. To map a quantum circuit for a specific quantum algorithm to quantum hardware, qubit mapping is an imperative technique based on the qubit topology. Due to the neighborhood constraint of qubit topology, the implementation of the quantum algorithm rightly, is essential for moving information around in a quantum computer. Swapping of qubits using a SWAP gate moves the quantum state between two qubits and solves the neighborhood constraint of qubit topology. Although, one needs to decompose the SWAP gate into three controlled-NOT gates to implement the SWAP gate efficiently, but unwillingly quantum cost with respect to the gate count and depth increases. In this paper, a formalism of moving quantum states without using SWAP operation is introduced. Moving quantum states through qubits have been attained with the adoption of temporary intermediate qudit states. This introduction of intermediate qudit states has exhibited a three times reduction in quantum cost with respect to the gate count and approximately two times reduction with respect to circuit depth compared to the state-of-the-art approach of the SWAP gate insertion. We also exhibit that the adoption of the intermediate qudit makes the approach sublimer than the existing works by obtaining a better fidelity. Furthermore, the proposed approach is generalized to any finite-dimensional quantum system.

I. INTRODUCTION

As it is experimentally quite established that the quantum computing system can be realized on various physical technologies, for example, continuous spin systems [1,2], superconducting transmon technology [3], nuclear magnetic resonance [4,5], photonic systems [6], an ion trap [7], topological quantum systems [8,9], and molecular magnets [10], the physical implementation of quantum algorithms [11] is now a blazing topic among the researchers for its asymptotic improvements [12]. Transistors of the classical computer deal with binary bits to accomplish information processing at the physical level. On the other hand, qubit technology is the base of quantum computers. A quantum system can have an infinite arity of discrete energy levels, and, hence, the fundamental physics behind the quantum system is not inherently binary. As per the real scenario, the impediment lies in the fact is that we need to control the system as per our requirements. The inclusion of additional discrete energy levels for the goal of computation enables us to realize the qudit technology quite predominantly, which makes the system more malleable with data storage and rapid processing of quantum information.

The first step towards implementation of a quantum algorithm is logic circuit synthesis. Since physical quantum computer only braces single-qubit gates and two-qubit gates [13], thus, it becomes evident that the logical circuit synthesis must be decomposed into single-qubit gates and two-qubit gates so as to implement the algorithm on real quantum hardware devices. Every physical quantum computer has its own architectural design and qubit topology. A logic circuit design using only single-qubit gates and two-qubit gates does not suffice to be implemented physically. For this reason, there is the qubit mapping or qubit placement algorithm [14–16] based on qubit topology, which makes the implementation on physical quantum devices a reality. The operation involving two-qubit gates are of most concern rather than single-qubit gates whereas mapping them on physical devices as the qubit topology may not support the placement of the required two physical qubits adjacently. To solve this constraint, ideally, SWAP gates [17,18] are used to move quantum states between two logical qubits. The idea is to exchange the qubits with repeated SWAP operations so that two logical qubits associated with two-qubit gates can arrive at two adjacent physical qubits, but some additional cost is incurred.

In this paper, we have aspired to reduce the additional quantum cost that is incurred for the SWAP insertion [19]. We propose a qubit-qudit approach [20–23] to move the quantum states through qubits to circumvent the SWAP operation. This is an approach and achieves optimized gate cost and depth. One can simply have a higher-dimensional quantum state for temporary use by easily introducing a discrete energy level. However, these higher-dimensional quantum states are only present as intermediate states in a qudit system, whereas the input and output states still remain qubits [24]. We introduce the $|2\rangle$ and $|3\rangle$ quantum states as temporary storage of ququad quantum systems without hindering the fundamental operation of initialization and measurement on physical devices since we are considering qubit systems where two quantum states have to be temporarily stored. It is kind of approach of moving quantum states through the qubit without SWAP

*abamitsaha@gmail.com
†asakc@caluniv.ac.in

insertion via intermediate qudits, which is later extended to d-dimensional quantum systems with the use of $|d\rangle$, $|d+1\rangle$, ..., $|2d-1\rangle$ quantum states as temporary storage. Our major contributions are the following:

(1) With the use of temporary intermediate qudit states, moving quantum states through qubits have been studied.

(2) These temporary intermediate qudit states help to reduce a significant number of quantum cost with respect to gate cost and circuit depth cost compared to the exchange of qubit states using the SWAP gate. Hence, we also show that the percentage increase in the probability of success is significant for the intermediate qudit approach.

(3) Furthermore, we claim that with the help of temporary intermediate higher-dimensional qudit states, quantum states can be moved through qudits in any dimensional quantum system or d-ary quantum systems with similar advancement with respect to quantum cost as binary quantum systems, which makes our approach generalized in nature.

The structure of the paper is as follows. Section II illustrates the SWAP gate and its usefulness. Section III exemplifies the methodology of moving quantum states through qubits using intermediate qudit with some example of circuit instances. Section IV exhibits how the proposed method can be extended to any finite-dimensional quantum system. Section V analyzes the circuit comparison between conventional and proposed work. Section VI highlights the error analysis of the proposed approach. Section VII captures our conclusions with a brief discussion.

II. BACKGROUND

The schematic to represent quantum algorithm or quantum program is known as a quantum circuit. Each line in the quantum circuit is denoted as a qubit and the operations, i.e., quantum gates are represented by different blocks on the line [13,25]. There are mainly three basic cost metrics of a quantum circuit in quantum computing, viz. qubit cost, quantum gate cost and count (single- or two-qubit gates only) and depth of a circuit. The qubit cost and the quantum gate count are the number of qubits and the quantum gates, respectively, that are presented in a circuit. In a circuit, the path length for every case is an integer, which represent the number of gates to be executed in that path. The longest path in a circuit is the depth of the circuit. Since all the qubits are not physically connected, the placement of the logical qubits needs to be rearranged to make them executable on the physical quantum devices. Fortunately, this can be performed quite comprehensibly by using SWAP gates. Let us discuss more about the SWAP gate.

A. SWAP gate

In Ref. [26], the authors have presented a SWAP gate implementation that interchanges the quantum states between two qubits. Let there be the quantum states of two qubits as $|\phi\rangle$ and $|\psi\rangle$, then the SWAP gate will work as

$$\text{SWAP}|\phi\rangle|\psi\rangle = |\psi\rangle|\phi\rangle. \tag{1}$$

Three controlled-NOT (CNOT) gates constitute the SWAP operation as in Fig. 1. CNOT is the two-qubit universal gate that
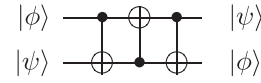

FIG. 1. CNOT swapping circuit.

has a control qubit, portrayed as a black dot ($\bullet$), and a target qubit, portrayed with the XOR symbol ($\oplus$). If the control qubit of a CNOT gate is in quantum state $|1\rangle$, the target qubit's value alters from $|0\rangle$ to $|1\rangle$ or/and from $|1\rangle$ to $|0\rangle$. The CNOT gate can be mathematically illustrated as

$$\text{CNOT}|x\rangle|y\rangle = |x\rangle|x \oplus y\rangle. \tag{2}$$

The XOR operation is mod 2 addition where target qubit is incremented by 1 (mod 2) only when the control qubit value is 1.

In following steps [Eqs. (3)–(5)], how the concatenation of three CNOT gates implements the SWAP operation is shown

$$|x\rangle|y\rangle \xrightarrow{\text{CNOT}_{q_1,q_0}} |x \oplus y\rangle|y\rangle, \tag{3}$$

$$|x \oplus y\rangle|y\rangle \xrightarrow{\text{CNOT}_{q_0,q_1}} |x \oplus y\rangle|y \oplus x \oplus y\rangle = |x \oplus y\rangle|x\rangle, \tag{4}$$

$$|x \oplus y\rangle|x\rangle \xrightarrow{\text{CNOT}_{q_1,q_0}} |x \oplus y \oplus x\rangle|x\rangle = |y\rangle|x\rangle. \tag{5}$$

Here, by convention, $\text{CNOT}_{i,j}$ is a CNOT gate controlled by qubit i and with qubit j as target. In this paper, qubits are labeled serially as $\{q_0, q_1, \ldots, q_n\}$. The unitary transformation of the quantum states that we have illustrated here must give a desired result even if the quantum states are superposed.

B. Qubit mapping problem

For explaining this qubit mapping problem with the help of SWAP insertion, we have considered an example as shown in Fig. 2(a). In Fig. 2(b), a three-qubit topology is used as the hardware platform. Two-qubit gates are executable on the following adjacent physical qubits: $\{P_0, P_1\}$, $\{P_1, P_2\}$, and not on $\{P_0, P_2\}$. Now, suppose we have a CNOT to be executed
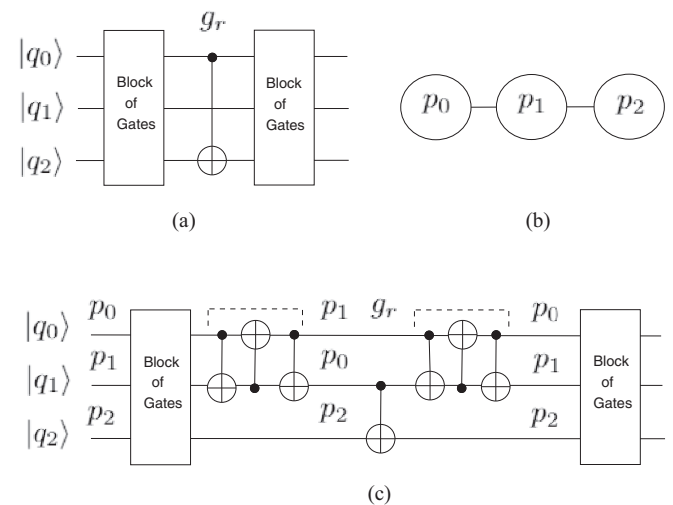

(a)

(b)

(c)

FIG. 2. (a) Example: circuit, (b) example: qubit topology, and (c) SWAP insertion.

on this three-qubit device. This quantum circuit consists of several other gates [as shown in Fig. 2(a) as a block of gates]. Assuming the initial logical-to-physical qubits mapping is $\{q_0 \longrightarrow P_0, q_1 \longrightarrow P_1, q_2 \longrightarrow P_2\}$. We can find that CNOT gate (g_r) as shown in Fig. 2(a) cannot be executed because the corresponding qubit pairs are not connected on the device. We need to change the qubit mapping during execution and make the CNOT gate executable.

To overcome this issue, we employ SWAP operation to change the qubit mapping by exchanging the states between two qubits. It consists of three CNOT gates as shown in Fig. 1. Figure 2(c) shows that the updated quantum circuit is now executable after we insert one SWAP operation between q_0 and q_1 as shown dotted. After the inserted SWAP, mapping is updated to $\{q_0 \longrightarrow P_1, q_1 \longrightarrow P_0, q_2 \longrightarrow P_2\}$. Now, the CNOT gate can be executed under this updated mapping. For further execution of the remaining block of gates, we need to again apply SWAP operation between q_0 and q_1 as shown dotted in Fig. 2(c) to get back to the previous logical-to-physical qubits mapping, which is $\{q_0 \longrightarrow P_0, q_1 \longrightarrow P_1, q_2 \longrightarrow P_2\}$.

With the introduction of additional SWAPs in the quantum circuit, all the two-qubit gate dependencies can be solved and a hardware-compliant circuit with unchanged original functionality is generated. Furthermore, insertion of SWAPs in the quantum circuit will lead to several problems because of the limitations of quantum devices. There is an increase in the number of operations in the circuit. The overall error rate increases as the operations are not perfect, and noise will also be introduced. There might also be an increase in the depth of the circuit, i.e., there will be an increase in the total execution time and due to qubit decoherence, there will be an accumulation of too much error. If we compare the original circuit and the updated circuit in Figs. 2(a) and 2(c), the number of gates increases from 1 to 7 and the circuit depth is also increased from 1 to 7. Significant overhead in terms of fidelity and execution time will be brought with additional SWAPs. Thus, in order to reduce the overall error rate as well as total execution time for the final hardware-complaint circuit, we look forward to discard the additional SWAPs.

III. MOVING QUBIT STATES VIA INTERMEDIATE QUDITS

The most important aspect of our proposed paper is the moving quantum states through qubits without SWAP so that overall error rate can be optimized. In this regard, the states $|2\rangle$ and $|3\rangle$ of higher-dimensional ququad systems have been used in the intermediate levels during the computation. Since we keep input and output as binary, it enables these circuit constructions to act similarly as any already existing binary qubit-only circuits. Figure 3 describes how this can be achieved for the circuit shown in Fig. 2(a) based on qubit topology as shown in Fig. 2(b).

Although physical systems in classical hardware are typically binary, but common quantum hardware, such as in superconducting and trapped ion computers, has an infinite spectrum of discrete energy levels [24]. Quantum hardware may be configured to manipulate the lowest four energy levels by operating on ququads. In general, such a computer could be configured to operate on any number of d levels. Qudit gates
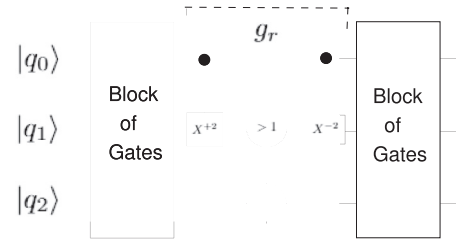

FIG. 3. Moving of a quantum state via intermediate qudits.

have already been successfully implemented [3,7] indicating it is possible to consider higher-level systems apart from qubit-only systems. Thus, the question of higher states beyond the standard two, being implemented and performed no longer stands strong. Since, conventional binary quantum gates [13] are not capable enough to get access to higher-dimensional quantum states, hence, new qubit-qudit quantum gates are needed to be introduced. First, let us consider an increment gate as C_X^{+2} (C: Control; X: NOT), where $+2$ denotes that the target qubit is incremented by 2 (mod 4) as a four-ary quantum system considered, only when the control qubit value is 1. For visualization of the C_X^{+2} gate, we have used a "black dot" ($\bullet$) to represent the control, and a "rectangle" ($\square$) to represent the targewt. X^{+2} in the target box represents the increment operator. The mathematical representation of the C_X^{+2} gate is as follows:

$$C_X^{+2} |x\rangle |y\rangle = \begin{cases} |x\rangle |(y+2)\%4\rangle, & \text{if } x = 1, \\ |x\rangle |y\rangle, & \text{otherwise.} \end{cases} \quad (6)$$

Since we are working with a qubit-qudit approach, this does not encapsulate the complete scenario, so we need to describe it with a matrix instead. The (8×8) unitary matrix representation of the C_X^{+2} gate is as follows:

$$C_X^{+2} = \begin{array}{c} \\ 00 \\ 01 \\ 02 \\ 03 \\ 10 \\ 11 \\ 12 \\ 13 \end{array} \begin{array}{cccccccc} 00 & 01 & 02 & 03 & 10 & 11 & 12 & 13 \\ \begin{pmatrix} 1 & 0 & 0 & 0 & 0 & 0 & 0 & 0 \\ 0 & 1 & 0 & 0 & 0 & 0 & 0 & 0 \\ 0 & 0 & 1 & 0 & 0 & 0 & 0 & 0 \\ 0 & 0 & 0 & 1 & 0 & 0 & 0 & 0 \\ 0 & 0 & 0 & 0 & 0 & 0 & 1 & 0 \\ 0 & 0 & 0 & 0 & 0 & 0 & 0 & 1 \\ 0 & 0 & 0 & 0 & 1 & 0 & 0 & 0 \\ 0 & 0 & 0 & 0 & 0 & 1 & 0 & 0 \end{pmatrix} \end{array}.$$

This gate operation is performed on the first and the second qubits as shown in Fig. 3, where the first qubit is the control, and the second qubit is the target. This upgrades the second qubit to $|2\rangle$ or $|3\rangle$ by availing the higher-dimensional Hilbert space as temporary storage if and only if the first qubit was $|1\rangle$.

Then, a conditional CNOT gate as $C_{X_c}^{+1}$, where c: conditional operator; and $+1$ denotes that the target qubit is incremented by 1 (mod 2) as the target qubit is in a binary quantum system if and only if the control qubit value is greater than 1 is applied to the target qubit, i.e., the third qubit and the second qubit as controls. In the schematic of the $C_{X_c}^{+1}$ gate, we have used ">1" in the conditional control circle (O) to represent the qubit control, and XOR ($\oplus$) in the target qubit to represent the conditional CNOT operator. The mathematical representation

of the $C_{X_c}^{+1}$ gate is as follows:

$$C_{X_c}^{+1} |x\rangle |y\rangle = \begin{cases} |x\rangle |(y+1)\%2\rangle, & \text{if } x > 1, \\ |x\rangle |y\rangle, & \text{otherwise.} \end{cases} \quad (7)$$

The (8×8) unitary matrix representation of the $C_{X_c}^{+1}$ gate is as follows:

$$C_{X_c}^{+1} = \begin{array}{c} \\ 00 \\ 01 \\ 10 \\ 11 \\ 20 \\ 21 \\ 30 \\ 31 \end{array} \begin{pmatrix} \begin{array}{cccccccc} 00 & 01 & 10 & 11 & 20 & 21 & 30 & 31 \\ 1 & 0 & 0 & 0 & 0 & 0 & 0 & 0 \\ 0 & 1 & 0 & 0 & 0 & 0 & 0 & 0 \\ 0 & 0 & 1 & 0 & 0 & 0 & 0 & 0 \\ 0 & 0 & 0 & 1 & 0 & 0 & 0 & 0 \\ 0 & 0 & 0 & 0 & 0 & 1 & 0 & 0 \\ 0 & 0 & 0 & 0 & 1 & 0 & 0 & 0 \\ 0 & 0 & 0 & 0 & 0 & 0 & 0 & 1 \\ 0 & 0 & 0 & 0 & 0 & 0 & 1 & 0 \end{array} \end{pmatrix}.$$

The conditional CNOT gate is executed only when the second qubit was $|2\rangle$ or $|3\rangle$ as expected, it would happen only when the first qubit was the $|1\rangle$ state. The controls are reinstated to their original states by a C_X^{-2} gate, i.e., inverse of the C_X^{+2} gate, which reverses the effect of the first gate. Thus, the $|2\rangle$ and $|3\rangle$ states from the four-ary quantum system can be used instead of SWAP to store temporary information, which is the most important aspect in this circuit composition. As shown in Fig. 3, the input of the circuit can be a form of $\sum_{x,y,t=0}^{1} \alpha_{x,y,t} |x\rangle |y\rangle |t\rangle$ where the first two are qubits q_0 and q_1, the target qubit t is q_2, $\alpha_{x,y,t} \in \mathbb{C}$, and $\sum_{x,y,t=0}^{1} |\alpha_{x,y,t}|^2 = 1$. Here, we show the action of the proposed gates [Eqs. (8)–(11)] on such a superposition by ignoring the block of gates for the sake of simplicity and understanding now and then,

$$\sum_{x=0,y,t}^{1} \alpha_{x,y,t} |x\rangle |y\rangle |t\rangle, \quad (8)$$

$$\xrightarrow{C_X^{+2}{}_{q_0,q_1}} \sum_{x=0,y,t} \alpha_{x=0,y,t} |0\rangle |y\rangle |t\rangle$$

$$+ \sum_{x=1,y,t} \alpha_{x=1,y,t} |1\rangle |(y+2)\%4\rangle |t\rangle, \quad (9)$$

$$\xrightarrow{C_{X_c}^{+1}{}_{q_1,q_2}} \sum_{x=0,y,t} \alpha_{x=0,y,t} |0\rangle |y\rangle |t\rangle$$

$$+ \sum_{x=1,y,t} \alpha_{x=1,y,t} |1\rangle |(y+2)\%4\rangle |(t+1)\%2\rangle, \quad (10)$$

$$\xrightarrow{C_X^{-2}{}_{q_0,q_1}} \sum_{x=0,y,t} \alpha_{x=0,y,t} |0\rangle |y\rangle |t\rangle$$

$$+ \sum_{x=1,y,t} \alpha_{x=1,y,t} |1\rangle |(y)\rangle |(t+1)\%2\rangle. \quad (11)$$

One more example of small four-qubit size [Fig. 4(a)] is used for explaining the changes in circuit realization if there is an increase in the number of qubit. In Fig. 4(b), a four-qubit device model is utilized as the hardware platform. Two-qubit gates are executable on the following physical qubit pairs: $\{P_0, P_1\}$, $\{P_1, P_2\}$, and $\{P_2, P_3\}$ not on $\{P_0, P_2\}$, $\{P_0, P_3\}$, and $\{P_1, P_3\}$. Let there be a CNOT gate controlled by qubit q_0 and
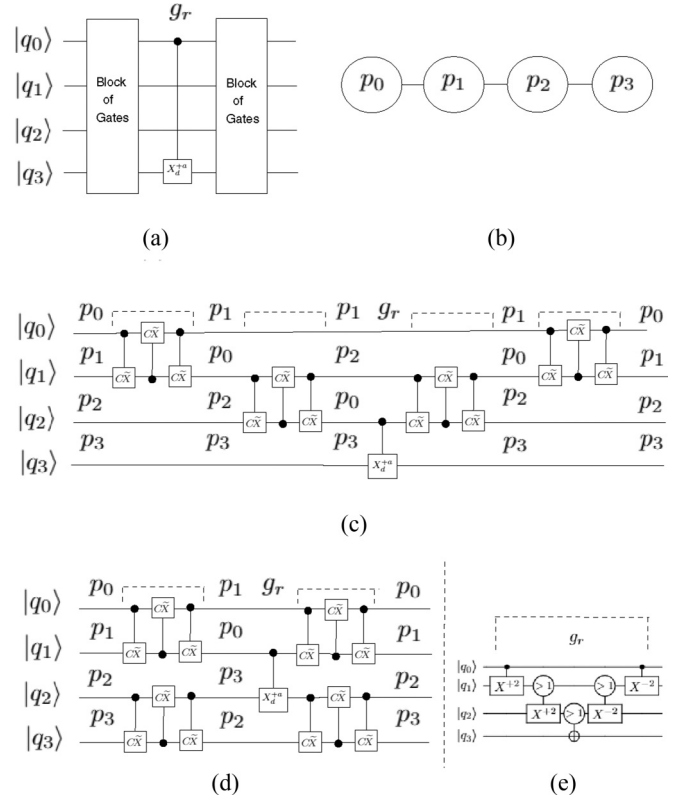

FIG. 4. (a) Example: circuit in binary quantum systems; (b) example: qubit topology; (c) SWAP insertion; (d) SWAP depth optimization; (e) proposed approach.

qubit q_3 as a target to be executed on this four-qubit device. Assuming the initial logical-to-physical qubits mapping is $\{q_0 \longrightarrow P_0, q_1 \longrightarrow P_1, q_2 \longrightarrow P_2\}$, the CNOT gate (g_r) as in Fig. 4(a) cannot be executed due to the corresponding qubit pairs being disconnected on the device. Hence, the qubit mapping needs to be changed during execution, and the CNOT gate must be made executable.

Conventionally, SWAP operation is needed to be employed for changing the qubit mapping with exchange of the quantum states between two qubits as in Fig. 2(c). Likewise, Fig. 4(c) shows that the updated quantum circuit is now executable after we insert two SWAP operations between "q_0 and q_1" and "q_1 and q_2" as shown dotted in Fig. 4(c). After the inserted SWAPs, logical qubit to physical qubit mapping is updated to $\{q_0 \longrightarrow P_1, q_1 \longrightarrow P_2, q_2 \longrightarrow P_0, q_3 \longrightarrow P_3\}$. Now, the CNOT gate can be executed following this updated mapping. For further execution of remaining block of gates, we need to again apply SWAP operation between q_0 and q_1 and "q_2 and q_3" as shown dotted in Fig. 4(c) to get back to the previous logical-to-physical qubits mapping. As per Gidney's work [27], the depth of the circuit shown in Fig. 4(c) can be optimized to a circuit shown in Fig. 4(d). This optimization shows that two series of SWAP gates can be implemented parally. Two parallely inserted SWAPs update the mapping to $\{q_0 \longrightarrow P_1, q_1 \longrightarrow P_0, q_2 \longrightarrow P_3, q_3 \longrightarrow P_2\}$. Now, the CNOT gate (g_r) can be executed under this updated mapping. Similarly, the mirror circuit can be applied parally as well, which improves the depth of a circuit but the gate cost remains

unchanged to the previous approach of circuit realization as shown in Fig. 4(c).

To eradicate the SWAP operation from Fig. 4(d), we need to introduce another new gate that is $C_{X_c}^{+2}$ atarget rectangular boxs the number of qubits have increased from 3 to 4. The $C_{X_c}^{+2}$ gate along with previously proposed C_X^{+2} and $C_{X_c}^{+1}$ gates will lead to execute the circuit shown in Fig. 4(a) based on the qubit topology as shown in Fig. 4(b). A conditional increment gate as $C_{X_c}^{+2}$, where $+2$ denotes that the target qubit is incremented by 2 (mod 4) as the four-ary quantum system considered, only when the control qubit value is greater than 1.

In the design of the gate, >1 has been used in the conditional control circle (O) to represent the qubit control, and X^{+2} in the target rectangular box ($\square$) to represent the increment operator. The mathematical representation of the $C_{X_c}^{+2}$ gate is as follows:

$$C_{X_c}^{+2} |x\rangle |y\rangle = \begin{cases} |x\rangle \, |(y+2)\%4\rangle, & \text{if } x > 1, \\ |x\rangle |y\rangle, & \text{otherwise.} \end{cases} \tag{12}$$

The (16×16) unitary matrix representation of the $C_{X_c}^{+2}$ gate is as follows:

$$C_{X_c}^{+2} =$$

	00	01	02	03	10	11	12	13	20	21	22	23	30	31	32	33
00	1	0	0	0	0	0	0	0	0	0	0	0	0	0	0	0
01	0	1	0	0	0	0	0	0	0	0	0	0	0	0	0	0
02	0	0	1	0	0	0	0	0	0	0	0	0	0	0	0	0
03	0	0	0	1	0	0	0	0	0	0	0	0	0	0	0	0
10	0	0	0	0	1	0	0	0	0	0	0	0	0	0	0	0
11	0	0	0	0	0	1	0	0	0	0	0	0	0	0	0	0
12	0	0	0	0	0	0	1	0	0	0	0	0	0	0	0	0
13	0	0	0	0	0	0	0	1	0	0	0	0	0	0	0	0
20	0	0	0	0	0	0	0	0	0	0	1	0	0	0	0	0
21	0	0	0	0	0	0	0	0	0	0	0	1	0	0	0	0
22	0	0	0	0	0	0	0	0	1	0	0	0	0	0	0	0
23	0	0	0	0	0	0	0	0	0	1	0	0	0	0	0	0
30	0	0	0	0	0	0	0	0	0	0	0	0	0	0	1	0
31	0	0	0	0	0	0	0	0	0	0	0	0	0	0	0	1
32	0	0	0	0	0	0	0	0	0	0	0	0	1	0	0	0
33	0	0	0	0	0	0	0	0	0	0	0	0	0	1	0	0

Figure 4(e) shows how the proposed gates can execute the circuit shown in Fig. 4(a) based on qubit topology as shown in Fig. 4(b) via temporary intermediate qudits. The initialization of Fig. 4(e) can be expressed as $\sum_{x,y,z,t=0}^{1} \alpha_{x,y,z,t} |x\rangle |y\rangle |z\rangle |t\rangle$ where the first three are qubits q_0, q_1, and q_2, and the target qubit t is q_3, $\alpha_{x,y,z,t} \in \mathbb{C}$, and $\sum_{x,y,z,t=0}^{1} |\alpha_{x,y,z,t}|^2 = 1$. Here, we show the action of a proposed gates on such a superposition [Eqs. (13)–(18)]. At first, the C_X^{+2} gate operation is performed on the first and the second qubits as illustrated in Eq. (14) where the first qubit is the control, and the second qubit is the target. This upgrades the second qubit to $|2\rangle$ or $|3\rangle$ by availing the higher-dimensional Hilbert space as temporary storage if and only if the first qubit was $|1\rangle$. Next, the $C_{X_c}^{+2}$ gate operation is performed on the second and the third qubits as illustrated in Eq. (15) where the second qubit is the control, and the third qubit is the target. This upgrades the third qubit to $|2\rangle$ or $|3\rangle$ by availing the higher-dimensional Hilbert space as temporary storage if and only if the second qubit was $|2\rangle$ or $|3\rangle$. Finally, a conditional CNOT $C_{X_c}^{+1}$ is applied to the target qubit q_3 and the third qubit as control as describes in Eq. (16). This gate will be executed only when the third qubit was $|2\rangle$ or $|3\rangle$ as expected and as discussed earlier, it would happen only when the first qubit was the $|1\rangle$ state. The controls are reinstated to their original states by applying the $C_{X_c}^{-2}$ gate followed by the C_X^{-2} gate, which reverses the effect of the first and second gates. Thus, the $|2\rangle$ and $|3\rangle$ states from the four-ary quantum system can be used instead of SWAP to store temporary information in q_1 and q_2 qubits, which is the most important aspect in this four-qubit circuit composition,

$$\sum_{x=0,y,z,t}^{1} \alpha_{x,y,z,t} |x\rangle |y\rangle |z\rangle |t\rangle, \tag{13}$$

$$\xrightarrow{C_X^{+2}{}_{q_0,q_1}} \sum_{x=0,y,z,t} \alpha_{x=0,y,z,t} |0\rangle |y\rangle |z\rangle |t\rangle + \sum_{x=1,y,z,t} \alpha_{x=1,y,z,t} |1\rangle |(y+2)\%4\rangle |z\rangle |t\rangle, \tag{14}$$

$$\xrightarrow{C_{X_c}^{+2}{}_{q_1,q_2}} \sum_{x=0,y,z,t} \alpha_{x=0,y,z,t} |0\rangle |y\rangle |z\rangle |t\rangle + \sum_{x=1,y,z,t} \alpha_{x=1,y,z} |1\rangle |(y+2)\%4\rangle |(z+2)\%4\rangle |t\rangle, \tag{15}$$

$$\xrightarrow{C_{X_c}^{+1}{}_{q_2,q_3}} \sum_{x=0,y,z,t} \alpha_{x=0,y,z,t} |0\rangle |y\rangle |z\rangle |t\rangle + \sum_{x=1,y,z,t} \alpha_{x=1,y,z,t} |1\rangle |(y+2)\%4\rangle |(z+2)\%4\rangle |(t+1)\%2\rangle, \tag{16}$$

$$\xrightarrow{C_{X_c}^{-2}{}_{q_1,q_2}} \sum_{x=0,y,z,t} \alpha_{x=0,y,z} |0\rangle |y\rangle |z\rangle |t\rangle + \sum_{x=1,y,z,t} \alpha_{x=1,y,z} |1\rangle |(y+2)\%4\rangle |z\rangle |(t+1)\%2\rangle, \tag{17}$$

$$\xrightarrow{C_{X}^{-2}{}_{q_0,q_1}} \sum_{x=0,y,z,t} \alpha_{x=0,y,z,t} |0\rangle |y\rangle |z\rangle |t\rangle + \sum_{x=1,y,z,t} \alpha_{x=1,y,z} |1\rangle |(y)\rangle |z\rangle |(t+1)\%2\rangle. \tag{18}$$

In Figs. 9(a) and 9(b), we have shown examples of a CNOT gate with five qubits and six qubits, respectively, which is portrayed in the Appendix. In these examples as in an earlier example, let us assume CNOT's control is in the first qubit, and the target is in the last qubit. For executing the CNOT gate, we need to move qubit states through the intermediate qubits by accessing the higher-dimensional Hilbert space. In Figs. 9(a) and 9(b), we show that these three proposed gates C_X^{+2}, $C_{X_c}^{+2}$, and $C_{X_c}^{+1}$ are sufficient to execute a CNOT gate in higher qubit systems as well. From this background, it can be inferred, for any higher n-qubit system ($q_1, q_2, q_3, \ldots, q_{n-1}, q_n$ where the two-qubit gate is involved between q_1 and q_n), the proposed three gates can be used for moving quantum states for physical implementation without the use of the SWAP gate. We can conclude that the C_X^{+2} gate is used between the first and the second qubits, i.e., q_1 and q_2, for intermediate operations, the $C_{X_c}^{+2}$ gate is used on $\{(q_2, q_3), (q_3, q_4), l \ldots, (q_{n-2}, q_{n-1})\}$, and finally $C_{X_c}^{+1}$ is executed with the control qubit q_{n-1} and target qubit q_n.

IV. MOVING d-DIMENSIONAL QUANTUM STATES VIA HIGHER-DIMENSIONAL QUDITS

In this section, we consider the implementation of our proposed qubit-qudit method generalized to any finite dimension as the qudit–higher-dimensional-qudit method. Qudit technology is concerned with d-ary quantum systems, where $d > 2$ [28,29]. We graduate to qudits for providing a larger state space and simultaneous multiple control operations, which in the long run reduce the circuit complexity and uplift the efficiency of quantum algorithms [30–32]. For example, N qubits can be depicted as $\frac{N}{\log_2 d}$ qudits, which straightway reduces a $\log_2 d$ factor from the run time of a quantum algorithm [33]. An akin construction of proposed binary gates using a qudit have been extended for the d-ary quantum system by generalizing the $C_{X_c}^{+2}$, C_X^{+2}, and $C_{X_c}^{+1}$ gates. The aim is to move the d-dimensional quantum states through qudits by accessing the higher-dimensional quantum space as temporary storage. As we have shown the binary quantum system needs to access $|2\rangle$ and $|3\rangle$ of the ququad system, likewise, it generalizes for a d-dimensional quantum system by accessing additional d-dimensional Hilbert space since d quantum states have to be temporarily stored with the use of $|d\rangle$, $|d+1\rangle$, \ldots, $|2d-1\rangle$ quantum states of the $2d$-dimensional
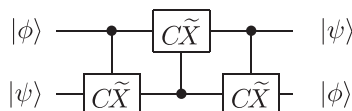
quantum system as temporary storage, we can avoid SWAP gate in the qudit system to get a solution of our objective. Before discussing more about our proposed method, let us enlighten about the SWAP gate in the qudit system [34–36].

SWAP gate in qudit systems

In Ref. [26], the author proposed a gate $\widetilde{CX}$, a generalization of the CNOT gate in qudit systems, which generally acts on qudits $|x\rangle$ and $|y\rangle$ from the basis $\{|0\rangle, |1\rangle, \ldots, |d-1\rangle\}$ so that

$$\widetilde{CX} |x\rangle |y\rangle = |x\rangle |-x-y\rangle. \tag{19}$$

$|-x-y\rangle$ denotes a state $|i\rangle$ in the range of $i = 0, \ldots, d-1$ with $i = -x - y \mod d$.

The SWAP gate shown in Fig. 1 has been extended to qudit systems using three $\widetilde{CX}$ gates, which is described in Fig. 5. If $\widetilde{CX}_{i,j}$ is a $\widetilde{CX}$ gate where the control is qudit i and the target

(a)   (b)
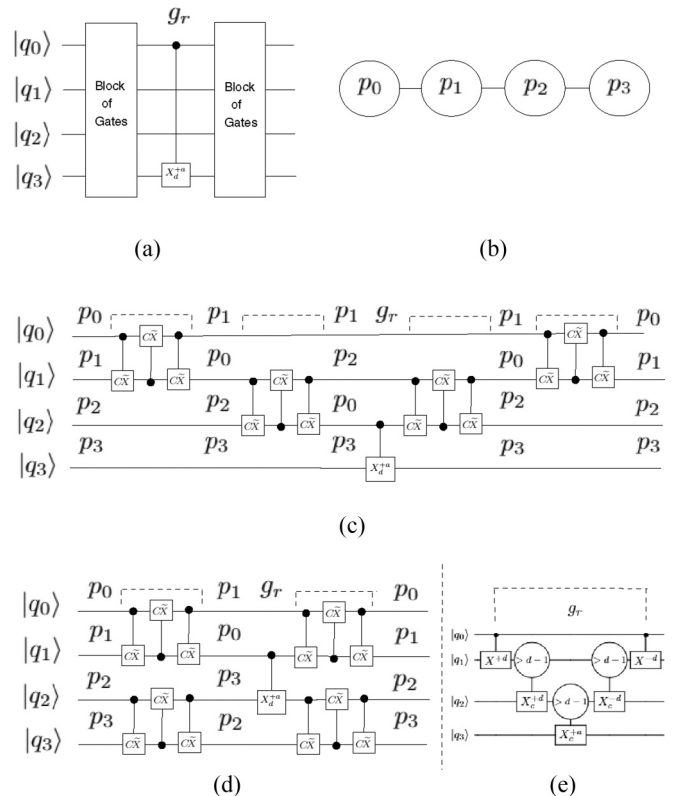

(c)

(d)   (e)

FIG. 6. (a) Example: circuit in d-ary quantum systems; (b) example: qudit topology; (c) SWAP insertion; (d) SWAP depth optimization; (e) proposed approach.

FIG. 5. Qudit swapping circuit.

qudit j, the qudit SWAP gate that is evolved through

$$|x\rangle |y\rangle \xrightarrow{\widetilde{CX}_{q_2,q_1}} |-x-y\rangle |y\rangle, \tag{20}$$

$$|-x-y\rangle |y\rangle \xrightarrow{\widetilde{CX}_{q_1,q_2}} |-x-y\rangle |x+y-y\rangle = |-x-y\rangle |x\rangle, \tag{21}$$

$$|-x-y\rangle |x\rangle \xrightarrow{\widetilde{CX}_{q_2,q_1}} |-x+x+y\rangle |x\rangle = |y\rangle |x\rangle. \tag{22}$$

This SWAP operation for qudit systems must be acted upon appropriately for any possible arbitrary superposed input qudit with quantum state from $\{|0\rangle, |1\rangle, \ldots, |d-1\rangle\}$.

As mentioned earlier, the proposed binary gates are needed to be generalized for d-ary quantum systems. Let us consider a generalized increment gate for d-ary quantum systems as C_X^{+d}, where $+d$ denotes that the target qudit is incremented by d (mod $2d$) as $2d$-ary quantum systems considered, if and only if the control qudit value is $d-1$. For visualization of the C_X^{+d} gate, we have used a black dot ($\bullet$) to represent the control, and a rectangle ($\square$) to represent the target. X^{+d} in the target box represents the increment operator. The mathematical representation of the C_X^{+d} gate is as follows:

$$C_X^{+d} |x\rangle |y\rangle = \begin{cases} |x\rangle |(y+d)\%2d\rangle, & \text{if } x = d-1; \\ |x\rangle |y\rangle, & \text{otherwise.} \end{cases} \tag{23}$$

A conditional increment gate can be extended to a generalized conditional increment gate for d-ary quantum systems as $C_{X_c}^{+d}$, where $+d$ denotes that the target qudit is incremented by d (mod $2d$) as $2d$-ary quantum systems considered, only when the control qudit value is greater than $d-1$. In the design of the $C_{X_c}^{+d}$ gate, "$>d-1$" has been used in the

conditional control circle (O) to represent the qudit control and "X_c^{+d}" in the target rectangular box ($\square$) to represent the increment operator. The mathematical representation of the $C_{X_c}^{+d}$ gate is as follows:

$$C_{X_c}^{+d} |x\rangle |y\rangle = \begin{cases} |x\rangle |(y+d)\%2d\rangle, & \text{if } x > d, \\ |x\rangle |y\rangle, & \text{otherwise.} \end{cases} \tag{24}$$

In a similar way, a conditional CNOT gate can be extended to d-ary quantum systems. The generalized conditional CNOT gate can be defined for d-ary quantum systems as $C_{X_c}^{+a}$, where $+a$ denotes that the target qudit is incremented by a (mod d) as d-ary quantum systems considered if and only if the control qudit value is greater than $d-1$ whereas $1 \leqslant a \leqslant d-1$. In the schematic of the $C_{X_c}^{+a}$ gate, we have used $>d-1$ in the conditional control circle (O) to represent the qudit control, and "X_c^{+a}" in the target rectangular box ($\square$) to represent the conditional CNOT operator. The mathematical representation of the $C_{X_c}^{+a}$ gate is as follows:

$$C_{X_c}^{+a} |x\rangle |y\rangle = \begin{cases} |x\rangle |(y+a)\%d\rangle, & \text{if } x > d, \\ |x\rangle |y\rangle, & \text{otherwise.} \end{cases} \tag{25}$$

Figure 6(e) shows how the proposed gates can execute the circuit shown in Fig. 6(a) based on qudit topology as shown in Fig. 6(b) via temporary intermediate higher-dimensional qudits. A conventional approach of executing the circuit having generalized CNOT gate for d-dimensional quantum systems shown in Fig. 6(a) using SWAP for qudit systems can be found in Figs. 6(c) and 6(d). The initialization of Fig. 6(e) can be expressed as $\sum_{x,y,z,t=0}^{d-1} \alpha_{x,y,z,t} |x\rangle |y\rangle |z\rangle |t\rangle$ where the first three are qudits q_0, q_1, and q_2 and the target qudit t is q_3, $\alpha_{x,y,z,t} \in \mathbb{C}$, and $\sum_{x,y,z,t=0}^{d-1} |\alpha_{x,y,z,t}|^2 = 1$. Here, we show the action of proposed gates on such a superposition [Eqs. (26)–(31)],

$$\sum_{x,y,z,t}^{d-1} \alpha_{x,y,z,t} |x\rangle |y\rangle |z\rangle |t\rangle, \tag{26}$$

$$\xrightarrow{C_X^{+d}{}_{q_0,q_1}} \sum_{x,y,z,t} \alpha_{x\neq d-1,y,z,t} |x \neq d-1\rangle |y\rangle |z\rangle |t\rangle + \sum_{x,y,z,t} \alpha_{x=d-1,y,z,t} |d-1\rangle |(y+d)\%2d\rangle |z\rangle |t\rangle, \tag{27}$$

$$\xrightarrow{C_{X_c}^{+d}{}_{q_1,q_2}} \sum_{x,y,z,t} \alpha_{x\neq d-1,y,z,t} |x \neq d-1\rangle |y\rangle |z\rangle |t\rangle + \sum_{x,y,z,t} \alpha_{x=d-1,y,z,t} |d-1\rangle |(y+d)\%2d\rangle |(z+d)\%2d\rangle |t\rangle, \tag{28}$$

$$\xrightarrow{C_{X_c}^{+a}{}_{q_2,q_3}} \sum_{x,y,z,t} \alpha_{x\neq d-1,y,z,t} |x\rangle |y\rangle |z\rangle |t\rangle + \sum_{x,y,z,t} \alpha_{x=d-1,y,z,t} |d-1\rangle |(y+d)\%2d\rangle |(z+d)\%2d\rangle |(t+a)\%d\rangle, \tag{29}$$

$$\xrightarrow{C_{X_c}^{-d}{}_{q_1,q_2}} \sum_{x,y,z,t} \alpha_{x\neq d-1,y,z,t} |x \neq d-1\rangle |y\rangle |z\rangle |t\rangle + \sum_{x,y,z,t} \alpha_{x=d-1,y,z,t} |d-1\rangle |(y+d)\%2d\rangle |z\rangle |(t+a)\%d\rangle, \tag{30}$$

$$\xrightarrow{C_X^{-d}{}_{q_0,q_1}} \sum_{x,y,z,t} \alpha_{x\neq d-1,y,z,t} |x \neq d-1\rangle |y\rangle |z\rangle |t\rangle + \sum_{x,y,z,t} \alpha_{x=d-1,y,z,t} |d-1\rangle |(y)\rangle |z\rangle |(t+a)\%d\rangle. \tag{31}$$

At first, the C_X^{+d} gate operation is performed on the first and the second qudits as illustrated in Eq. (27) where first qudit is the control, and the second qudit is the target. This upgrades the second qudit to $|d\rangle$ or $|d+1\rangle$ or $\cdots |2d-1\rangle$ by availing the higher-dimensional space as temporary storage if and only if the first qudit was $|d-1\rangle$. Next, the $C_{X_c}^{+d}$ gate operation is

performed on the second and the third qudits as illustrated in Eq. (28) where second qudit is the control, and the third qudit is the target. This upgrades the third qudit to $|d\rangle$ or $|d+1\rangle$ or $\cdots |2d-1\rangle$ by availing the higher-dimensional space as temporary storage if and only if the second qudit was $|d\rangle$ or $|d+1\rangle$ or $\cdots |2d-1\rangle$. Finally, a generalized conditional

TABLE I. Comparative analysis.

Number of qubits and qudits involved in between two-qubit and qudit gates	Proposed work		Conventional work	
	Gate count	Depth	Gate count	Depth
3	3	3	7	7
4	5	5	13	7
5	7	7	19	13
6	9	9	25	13
7	11	11	31	19
8	13	13	37	19
9	15	15	43	25
10	17	17	49	25
n	$2(n-2)+O(1)$	$2(n-2)+O(1)$	$6(n-2)+O(1)$	$6(\lceil \frac{n}{2} \rceil -1)+O(1)$

CNOT $C_{X_c}^{+a}$ is applied to the target qudit q_3, and the third qudit q_2 as the control as described in Eq. (29). This gate will be executed only when the third qudit was $|d\rangle$ or $|d+1\rangle$ or $\cdots |2d-1\rangle$, it would happen only when the first qudit was the $|d-1\rangle$ state. The controls are reinstated to their original states by applying the $C_{X_c}^{-d}$ gate followed by the C_X^{-d} gate, which reverses the effect of the first and second gates. Thus, the $|d\rangle$ or $|d+1\rangle$ or $\cdots |2d-1\rangle$ state from $2d$-ary quantum systems can be used instead of SWAP to store temporary information in q_1 and q_2 qudits as discussed earlier in binary quantum systems as well. As in binary quantum systems, for any higher n-qudit systems, the proposed three gates can be used for moving quantum states for physical implementation without the use of a SWAP gate.

V. COMPARATIVE ANALYSIS

In previous sections, we tried to implement a universal two-qubit or two-qudit CNOT gate in which qubits and qudits are not adjacent to each other with respect to qubit and qudit topology. We considered the generalized CNOT gate as an example to establish our claim for the simplicity of understanding, even though our approach stands good for any other two-qubit or two-qudit gate with simple modification in the proposed gates as per unitary operation at the target. To make them adjacent, the conventional approach is to insert the SWAP gates between two qubits and qudits. The optimal gate cost of SWAP and its mirror circuit is six CNOT gates using the conventional decomposition-based approach [27] where three qubits are involved as shown in Fig. 2. This is also legitimate for any d-dimensional quantum systems, but the only difference is $\widetilde{CX}$ replaces CNOT here. Correspondingly, the optimal depth cost of SWAP and its mirror circuit is six using the conventional decomposition-based approach for any d-ary quantum systems. Furthermore, a four-qubits and a four-qudits circuit implementation have been illustrated in Figs. 4 and 6, respectively. Two SWAP operations have to be inserted to make the circuit executable is shown in Figs. 4 and 6. A conventional optimization technique yields the depth constant as compared to the three qubit examples as shown in Fig. 2. Albeit, the gate count increases by six for additional two SWAP insertion. The conventional approach of SWAP insertion generalizes the gate cost and the depth for any n-qubit and qudit circuit.

For the execution of one two-qubit gate on the n-qubit and qudit circuit where $n-2$ SWAP insertions are required to make the control and the target qubit and qudit adjacent, the gate count of the updated circuit becomes $6(n-2)+O(1)$ and the depth of the circuit becomes $6(\lceil \frac{n}{2} \rceil -1)+O(1)$ [where $O(1)$ is for two-qubit and qudit gates that have to be executed]. As shown in Table I, we achieved a whooping reduction to $2(n-2)+O(1)$ as the gate count and $2(n-2)+O(1)$ as the depth compared to the convention work whereas n qubits and qudits are involved for a two-qubit and qudit gate. Figure 7 shows that the proposed paper outperforms conventional state-of-the-art techniques with respect to gate count and circuit depth. Thus, it can be concluded that for the employment of intermediate qudits, our approach supersedes the current techniques on the basis of circuit depth and circuit robustness. The effect of various error models on our proposed approach is discussed next.

VI. ERROR ANALYSIS

Any finite-dimensional quantum system is susceptible to errors due to the decoherence of the system or noisy gates. It has already been shown that other than binary systems, using more higher-dimensional states cause the system to have more errors [24,37]. The impact of these noises on the proposed approach has been thoroughly investigated in this section. Although the introduction of qudits increases noise, the overall error probability of the proposed approach is lower than that of the earlier SWAP decomposition [27] since the number of gate count and depth is optimized.

A. Error model

The generalized quantum error or noise model is for the gate and relaxation errors [24], which can be expressed by the Kraus operator formalism [11]. If the density-matrix representation of a (pure) quantum state is $\sigma = |\Psi\rangle \langle \Psi|$, the evolution of this state for any channel is represented as the function $\mathcal{E}(\sigma)$,

$$\mathcal{E}(\sigma) = \mathcal{E}(|\Psi\rangle \langle \Psi|) = \sum_i K_i \sigma K_i^{\dagger}, \qquad (32)$$
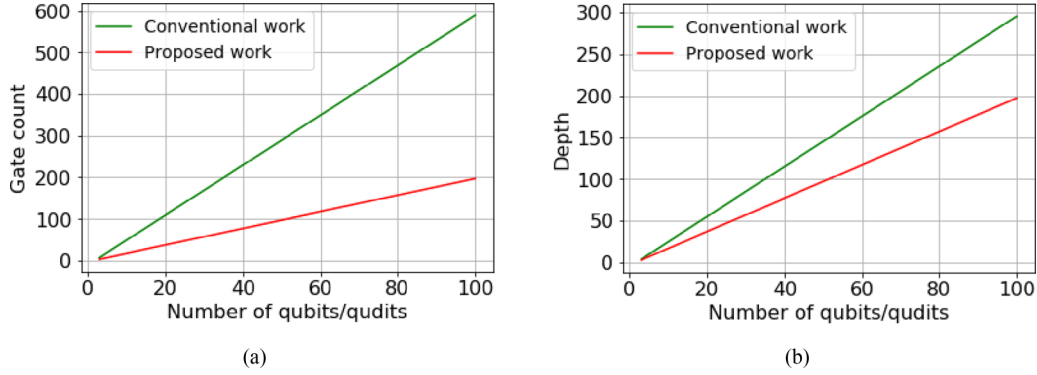
FIG. 7. (a) Gate count vs number of qubits and qudits for proposed work (lower curve) and conventional work (upper curve), (b) circuit depth vs number of qubits and qudits for proposed work (lower curve) and conventional work (upper curve).

where K_i's are called the Kraus operators and $K_i^\dagger$ is the matrix conjugate transpose of K_i, $\forall i$. The Kraus operator formulation represents the evolution of a state under a noise model. The Kraus operators, for example, are simply the Pauli matrices in the depolarization noise model.

1. Gate error

Since this paper only deals with two-qubit and qudit gates, in this section, only two-qubit and qudit gate errors are considered. In a conventional binary quantum system, there are four possible error channels for a quantum gate, which can be expressed as products of the two Pauli matrices, a NOT gate $X = \begin{pmatrix} 0 & 1 \\ 1 & 0 \end{pmatrix}$, and a phase gate $Z = \begin{pmatrix} 1 & 0 \\ 0 & -1 \end{pmatrix}$. The possible error channels are as follows: (i) no-error $X^0 Z^0 = I$, (ii) the phase flip which is the product $X^0 Z^1$, (iii) the bit flip which is $X^1 Z^0$, and (iv) the phase + bit flip channel given by $X^1 Z^1$. A noisy gate is modeled as an ideal gate followed by an unwanted Pauli operator [38]. In other words, a two-qubit gate is followed by an unwanted Pauli $\in \{I, X, Y, Z\}^{\otimes 2} \setminus \{I, I\}$ with probability $p_i p_j$, where $i, j \in \{x, y, z\}$.

For two-qubit gates, an unwanted Pauli operator can occur on each of the two qubits after the gate operation. Therefore, there are $2^4 - 1$ ways (excluding the identity operation on both qubits) in which a gate can be noisy. If p_2 is the probability of two-qubit gate errors, then the evolution of the system under noisy two-qubit operations is represented as in Eq. (33),

$$\mathcal{E}(\sigma) = [1 - (2^4 - 1)p_2]\sigma + \sum_{jklm \in \{0,1\}^2 \setminus 0*2} p_{jklm} K_{jklm} \sigma K_{jklm}^\dagger,$$

(33)

where $p_{jklm} = p_{jk} p_{lm}$. The probability that the density matrix remains error free is independent of whether the underlying depolarizing channel is symmetric or asymmetric. Rather, it depends on the total probability of error.

Our proposed approach here deals with two-ququad gates only on quaternary quantum systems. In general, our proposed method uses up to four dimensions. Therefore, for a four-dimensional system, the error in our system scales as $O(4^4)$

as shown in Eq. (34),

$$\mathcal{E}(\sigma) = \{1 - (4^4 - 1)p_2\}\sigma + \sum_{\substack{jklm \in \\ \{0-2,\ldots,3\}^4 \setminus 0000}} p_{jklm} K_{jklm} \sigma K_{jklm}^\dagger.$$

(34)

Hence, we conclude that the decrease in the probability of no error for two-ququad gates due to the usage of higher dimensions for quaternary systems is $1 - 255 p_2$ as compared to $1 - 15 p_2$ for conventional binary systems.

Similarly, in a d-ary system for two-qudit gates, an unwanted Pauli operator can occur on each of the two qudits after the gate operation. Therefore, there are $d^4 - 1$ ways (excluding the identity operation on both qudits) in which a gate can be noisy. If p_2 is the probability of two-qudit gate errors, then the evolution of the system under noisy two-qudit operations is represented as in Eq. (35),

$$\mathcal{E}(\sigma) = [1 - (d^4 - 1)p_2]\sigma + \sum_{jklm \in \{0,1\}^d \setminus 0*d} p_{jklm} K_{jklm} \sigma K_{jklm}^\dagger,$$

(35)

where $p_{jklm} = p_{jk} p_{lm}$. The probability that the density matrix remains error free is independent of whether the underlying depolarizing channel is symmetric or asymmetric. Rather, it depends on the total probability of error.

Since our proposed approach deals with two-qudit gates only on higher-dimensional quantum systems. Our proposed method uses up to $2d$ dimensions. Therefore, for a d-dimensional system, the error in our system scales as $O(2d)^4$ as shown in Eq. (36),

$$\mathcal{E}(\sigma) = \{1 - [(2d)^4 - 1]p_2\}\sigma$$
$$+ \sum_{\substack{jklm \in \\ \{0-2,\ldots,d+1\}^4 \setminus 0000}} p_{jklm} K_{jklm} \sigma K_{jklm}^\dagger.$$ (36)

Similarly, under this noise model, two-qudit gates in $(2d)$-ary quantum systems are $\{1 - [(2d)^4 - 1]p_2\}/[1 - (d^4 - 1)p_2]$ times less reliable than two-qudit gates in d-ary quantum systems.

2. Idle error

In quantum devices, idle errors mainly focus on the relaxation from higher- to lower-energy levels. Amplitude damping

is another name for this. This noise channel takes ququads to lower states in an irreversible manner. For qubits, the only amplitude damping channel is from $|1\rangle$ to $|0\rangle$, and we denote this damping probability as λ_1. For qubits, the Kraus operators for amplitude damping are as follows:

$$K_0 = \begin{pmatrix} 1 & 0 \\ 0 & \sqrt{1-\lambda_1} \end{pmatrix} \quad \text{and} \quad K_1 = \begin{pmatrix} 0 & \sqrt{\lambda_1} \\ 0 & 0 \end{pmatrix}. \quad (37)$$

For ququads, we also model damping from $|3\rangle$ to $|0\rangle$, which occurs with probability λ_3. For ququads, the Kraus operator for amplitude damping can be modeled as

$$K_0 = \begin{pmatrix} 1 & 0 & 0 & 0 \\ 0 & \sqrt{1-\lambda_1} & 0 & 0 \\ 0 & 0 & \sqrt{1-\lambda_2} & 0 \\ 0 & 0 & 0 & \sqrt{1-\lambda_3} \end{pmatrix},$$

$$K_1 = \begin{pmatrix} 0 & \sqrt{\lambda_1} & 0 & 0 \\ 0 & 0 & 0 & 0 \\ 0 & 0 & 0 & 0 \\ 0 & 0 & 0 & 0 \end{pmatrix}, \quad K_2 = \begin{pmatrix} 0 & 0 & \sqrt{\lambda_2} & 0 \\ 0 & 0 & 0 & 0 \\ 0 & 0 & 0 & 0 \\ 0 & 0 & 0 & 0 \end{pmatrix} \text{ and,}$$

$$K_3 = \begin{pmatrix} 0 & 0 & 0 & \sqrt{\lambda_3} \\ 0 & 0 & 0 & 0 \\ 0 & 0 & 0 & 0 \\ 0 & 0 & 0 & 0 \end{pmatrix}. \quad (38)$$

For qudits, we also model damping from $|2d-1\rangle$ to $|0\rangle$, which occurs with probability λ_{2d-1}. For qudits, the Kraus operator for amplitude damping can be modeled as

$$K_0 = \begin{pmatrix} 1 & 0 & 0 & \cdots & 0 \\ 0 & \sqrt{1-\lambda_1} & 0 & \cdots & 0 \\ 0 & 0 & \sqrt{1-\lambda_2} & \cdots & 0 \\ \vdots & \vdots & \vdots & \ddots & \vdots \\ 0 & 0 & 0 & \cdots & \sqrt{1-\lambda_{2d-1}} \end{pmatrix},$$

$$K_1 = \begin{pmatrix} 0 & \sqrt{\lambda_1} & 0 & \cdots & 0 \\ 0 & 0 & 0 & \cdots & 0 \\ 0 & 0 & 0 & \cdots & 0 \\ \vdots & \vdots & \vdots & \ddots & \vdots \\ 0 & 0 & 0 & \cdots & 0 \end{pmatrix},$$

$$\cdots K_{d-1} = \begin{pmatrix} 0 & 0 & 0 & \cdots & \sqrt{\lambda_{2d-1}} \\ 0 & 0 & 0 & \cdots & 0 \\ 0 & 0 & 0 & \cdots & 0 \\ \vdots & \vdots & \vdots & \ddots & \vdots \\ 0 & 0 & 0 & \cdots & 0 \end{pmatrix}. \quad (39)$$

In each Kraus operator K_i, the value of $\lambda_i \propto \exp(-t/T_{1_i})$, where t is the duration of the computation, and T_{1_i}'s are the relaxation time. We have qubit quantum devices, where $T_{1_1} \simeq 100 \, \mu s$ in some higher-end IBM quantum devices [39]. As per the state-of-the-art qudit device [40], we have the value of $30 \, \mu s$ for qutrit (T_{1_2}) and ququad (T_{1_3}) quantum devices. However, due to the lack of qudit quantum computers, we do not have explicit values of other T_{1_i}'s for more higher-dimensional systems. Nevertheless, the length of time depends on the circuit depth. As a result, by improving the circuit depth with the proposed approach, idle errors are reduced. Therefore, since
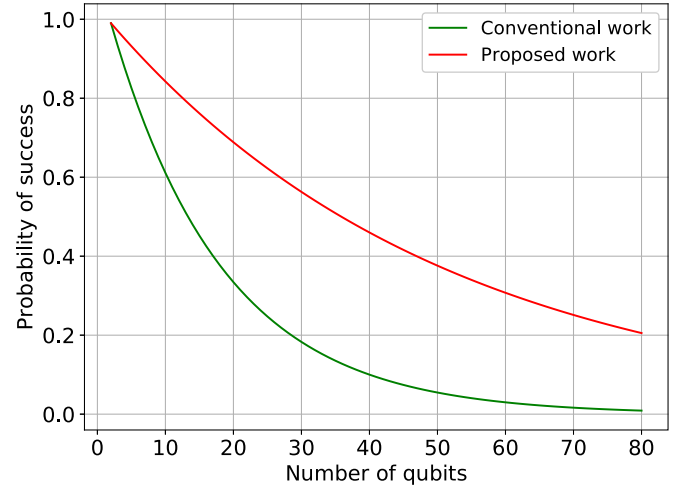

FIG. 8. Probability of success for the proposed method (upper curve) vs the conventional method (lower curve).

depth has been reduced, the decoherence owing to our employed approach is significantly lower than the conventional approach.

B. Analysis of success probability

In this section, we have considered the method in Ref. [27] with SWAP and our method in this article without SWAP to investigate the probability of success whereas moving quantum states in a circuit. The number of gates and depth of the circuit for the method in Ref. [27], and our proposed one is already depicted in Table I. As explained in previous subsections, small errors in quantum circuit gates can be characterized as an ideal gate followed by an undesirable Pauli operator. Instead of comparing the probability of minor circuit errors, we compare the probability of the circuit remaining error free (probability of success) as per Ref. [41] for the approach in Ref. [27] and our proposed approach without sacrificing generality.

The generalized formula for probability of success (P_{success}) described in Refs. [37,41] is the product that the individual components do not fail. In other words,

$$P_{\text{success}} = \Pi_{\text{gates}}[(P_{\text{success of gate}})^{\text{number of gates}} e^{-(\text{depth}/T_1)}], \quad (40)$$

where the first term's product is the likelihood of all types of gates incorporated (two qubit and two qudit in our case), and the second term is the probability of no ideal error.

Current quantum devices are mostly binary, and the probabilities of two-qubit gates in the IBMQ quantum devices are in the range of 10^{-2} [39]. Moreover, the time T_{1_1} of most of the IBM quantum devices are in the range of $100 \, \mu s$. However, in Ref. [40], the authors experimentally showed that the value of T_{1_3} for each quaternary gate is $30 \, \mu s$, which we have also assumed for our paper. We assume that the probability of error of each two-qubit and two-ququad gates is 10^{-2}. We also consider that the time T_{1_1} is $100 \, \mu s$ and T_{1_3} is $30 \, \mu s$ for our simulation.

In Fig. 8, we exhibit the probability of success for the method of Ref. [27] (which we label as conventional work) and our proposed paper. We find that our proposed technique

produces much fewer errors than the approach in Ref. [27]. This is due to the fact that our approach has fewer gates and the circuit is shallower. Although our approach employs a few ququad gates, which have a higher error probability due to the curse of dimensionality, our technique is superior due to the overall large reduction in gate count and depth. In fact, for $n = 80$ in a circuit where n is the number of qubits involved for a two-qubit gate, our proposed approach has a probability of success of $\simeq 0.21$, whereas that of Ref. [27] has a probability of success of $\simeq 0.01$. Therefore, we obtain a percentage decrease in the probability of error by $\simeq 20\%$ for $n = 80$. Thus, it can be concluded that the conventional method attain approximately 100% error for $n = 80$ in a circuit, whereas our method yields less erroneous results for $n = 80$ and above in a circuit.

VII. CONCLUSION

In this paper, we proposed a qubit-qudit approach to move the quantum states through qubits to eradicate the swap operation. The higher-dimensional quantum states are used as intermediate states in a qudit system, whereas the input and output states still remain qubits to solve the nearest-neighbor problem. We introduced the $|2\rangle$ and $|3\rangle$ quantum states as temporary storage of ququad quantum systems without hampering the fundamental operation of initialization and measurement on physical devices. Later on the extension of the proposed approach to d-dimensional quantum systems with the use of $|d\rangle, |d + 1\rangle, l \ldots, |2d - 1\rangle$ quantum states of $2d$-ary quantum systems as temporary storage has been addressed. For this approach, we achieved an optimized gate cost and depth with reduction to $2(n - 2) + O(1)$ as compared to the conventional work whereas n qubits and qudits are involved for a two-qubit and qudit gate for this problem. Through numerical analysis, we established that even though the use of qudits increases error since the number of gate count and the depth are both reduced the overall error probability of the proposed approach is lower than the existing ones. The impact of various error models on the proposed approach is discussed next.
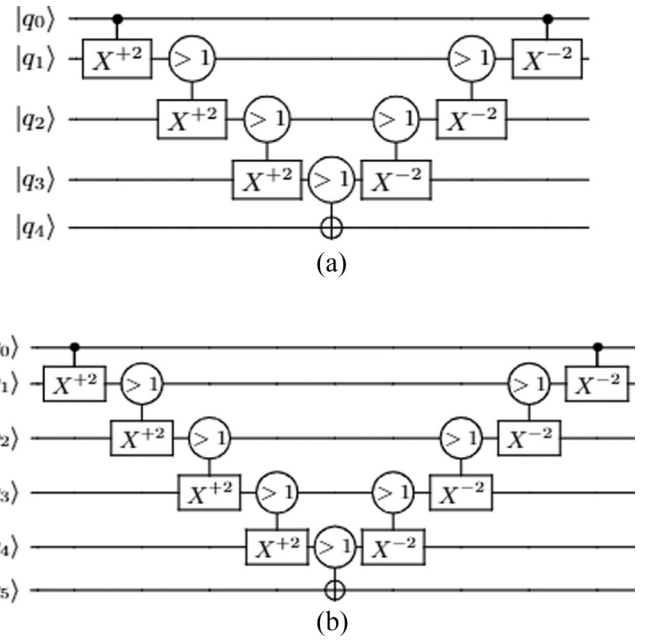

(a)

(b)

FIG. 9. (a) Five-qubit circuit and (b) six-qubit circuit.

In a future scope of this paper, we would like to mitigate the error that might happen due to the accessibility of higher-dimensional space as temporary storage. We would further like to apply our proposed approach to the existing qubit mapping algorithms to demonstrate the usefulness of our approach with the benchmarks circuits. In the near future, it can also be investigated that the proposed approach may give some advantage in quantum communication as SWAPs are involved there [42–44]. With the evolution of qudit-supported quantum hardware, we would like to validate our designs in the near future. The simulation of the proposed circuits for the verification is carried out on thr Google Colaboratory platform [45] and the code is available in Ref. [46].

APPENDIX: CNOT GATE WITH A HIGHER NUMBER OF QUBITS

Here, we have portrayed examples of a CNOT gate with five qubits and six qubits, respectively, in Figs. 9(a) and 9(b).

[1] S. D. Bartlett, H. de Guise, and B. C. Sanders, Quantum encodings in spin systems and harmonic oscillators, Phys. Rev. A **65**, 052316 (2002).

[2] M. R. A. Adcock, P. Høyer, and B. C. Sanders, Quantum computation with coherent spin states and the close Hadamard problem, Quant. Info. Proc. **15**, 1361 (2016).

[3] J. Koch, T. M. Yu, J. Gambetta, A. A. Houck, D. I. Schuster, J. Majer, A. Blais, M. H. Devoret, S. M. Girvin, and R. J. Schoelkopf, Charge-insensitive qubit design derived from the Cooper pair box, Phys. Rev. A **76**, 042319 (2007).

[4] S. Dogra, Arvind, and K. Dorai, Determining the parity of a permutation using an experimental NMR qutrit, Phys. Lett. A **378**, 3452 (2014).

[5] Z. Gedik, I. A. Silva, B. Çakmak, G. Karpat, E. L. G. Vidoto, D. O. Soares-Pinto, E. R. deAzevedo, and F. F. Fanchini, Computational speed-up with a single qudit, Sci. Rep. **5**, 14671 (2015).

[6] X. Gao, M. Erhard, A. Zeilinger, and M. Krenn, Computer-Inspired Concept for High-Dimensional Multipartite Quantum Gates, Phys. Rev. Lett. **125**, 050501 (2020).

[7] A. B. Klimov, R. Guzmán, J. C. Retamal, and C. Saavedra, Qutrit quantum computer with trapped ions, Phys. Rev. A **67**, 062313 (2003).

[8] S. X. Cui and Z. Wang, Universal quantum computation with metaplectic anyons, J. Math. Phys. **56**, 032202 (2015).

[9] S. X. Cui, S.-M. Hong, and Z. Wang, Universal quantum computation with weakly integral anyons, Quant. Info. Proc. **14**, 2687 (2015).

[10] M. N. Leuenberger and D. Loss, Quantum computing in molecular magnets, Nature (London) **410**, 789 (2001).

[11] M. A. Nielsen and I. L. Chuang, *Quantum Computation and Quantum Information* (Cambridge University Press, Cambridge, UK, 2010).

[12] J. Preskill, Quantum computing in the NISQ era and beyond, Quantum **2**, 79 (2018).

[13] A. Barenco, C. H. Bennett, R. Cleve, D. P. DiVincenzo, N. Margolus, P. Shor, T. Sleator, J. A. Smolin, and H. Weinfurter, Elementary gates for quantum computation, Phys. Rev. A **52**, 3457 (1995).

[14] A. Zulehner, A. Paler, and R. Wille, *Efficient Mapping of Quantum Circuits to the IBM QX Architectures, 2018* (IEEE, Piscataway, NJ, 2018), pp. 1135–1138.

[15] G. Li, Y. Ding, and Y. Xie, Tackling the qubit mapping problem for NISQ-Era quantum devices, in *Proceedings of the Twenty-Fourth International Conference on Architectural Support for Programming Languages and Operating Systems* (Association for Computing Machinery, New York, NY, 2019), pp. 1001–1014.

[16] B. Tan and J. Cong, Optimal layout synthesis for quantum computing, in *Proceedings of the 39th International Conference on Computer-Aided Design, ICCAD '20* (Association for Computing Machinery, New York, NY, 2020).

[17] L.-M. Liang and C.-Z. Li, Realization of quantum SWAP gate between flying and stationary qubits, Phys. Rev. A **72**, 024303 (2005).

[18] G. A. Paz-Silva, S. Rebić, J. Twamley, and T. Duty, Perfect Mirror Transport Protocol with Higher Dimensional Quantum Chains, Phys. Rev. Lett. **102**, 020503 (2009).

[19] C. Wilmott, A generalized quantum SWAP gate, arXiv:0811.1684.

[20] T. C. Ralph, K. J. Resch, and A. Gilchrist, Efficient Toffoli gates using qudits, Phys. Rev. A **75**, 022313 (2007).

[21] B. Lanyon, M. Barbieri, M. Almeida, T. Jennewein, T. Ralph, K. Resch, G. Pryde, J. O'Brien, A. Gilchrist, and A. White, Simplifying quantum logic using higher-dimensional Hilbert spaces, Nat. Phys. **5**, 134 (2009).

[22] T. Bækkegaard, L. Kristensen, N. Loft, C. Andersen, D. Petrosyan, and N. Zinner, Realization of efficient quantum gates with a superconducting qubit-qutrit circuit, Sci. Rep. **9**, 13389 (2019).

[23] W.-D. Li, Y.-J. Gu, K. Liu, Y.-H. Lee, and Y.-Z. Zhang, Efficient universal quantum computation with auxiliary Hilbert space, Phys. Rev. A **88**, 034303 (2013).

[24] P. Gokhale, J. M. Baker, C. Duckering, N. C. Brown, K. R. Brown, and F. T. Chong, Asymptotic improvements to quantum circuits via qutrits, in *Proceedings of the 46th International Symposium on Computer Architecture, 2019* (ACM, New York, 2019), pp. 554–566.

[25] X. Wang, Continuous-variable and hybrid quantum gates, J. Phys. A **34**, 9577 (2001).

[26] J. C. Garcia-Escartin and P. Chamorro-Posada, A SWAP gate for qudits, Quant. Inf. Proc. **12**, 3625 (2013).

[27] C. Gidney, Breaking down the quantum SWAP (2017).

[28] A. Muthukrishnan and C. R. Stroud, Jr., Multivalued logic gates for quantum computation, Phys. Rev. A **62**, 052309 (2000).

[29] Y. M. Di and H. R. Wei, Synthesis of multivalued quantum logic circuits by elementary gates, Phys. Rev. A **87**, 012325 (2013).

[30] Y. Cao, S.-G. Peng, C. Zheng, and G. Long, Quantum fourier transform and phase estimation in qudit system, Commun. Theor. Phys. **55**, 790 (2011).

[31] S. S. Ivanov, H. S. Tonchev, and N. V. Vitanov, Time-efficient implementation of quantum search with qudits, Phys. Rev. A **85**, 062321 (2012).

[32] A. Saha, S. B. Mandal, D. Saha, and A. Chakrabarti, One-dimensional lazy quantum walk in ternary system, IEEE Transactions on Quantum Engineering, **2**, 1 (2021).

[33] Y. Wang, Z. Hu, B. C. Sanders, and S. Kais, Qudits and high-dimensional quantum computing, Front. Phys. **8**, 589504 (2020).

[34] S. Balakrishnan, Various constructions of qudit SWAP gate, Phys. Res. Int. **2014** 479320 (2014).

[35] C. Wilmott, On swapping the states of two qudits, arXiv:1101.4159.

[36] C. Wilmott and P. R. Wild, Towards an optimal SWAP gate, Quant. Inf. Proc. **13**, 1467 (2014).

[37] A. Saha, R. Majumdar, D. Saha, A. Chakrabarti, and S. Sur-Kolay, Asymptotically improved circuit for a *d*-ary Grover's algorithm with advanced decomposition of the *n*-qudit Toffoli gate, Phys. Rev. A **105**, 062453 (2022).

[38] A. G. Fowler, M. Mariantoni, J. M. Martinis, and A. N. Cleland, Surface codes: Towards practical large-scale quantum computation, Phys. Rev. A **86**, 032324 (2012).

[39] IBM Quantum, https://quantum-computing.ibm.com/ (2021).

[40] L. E. Fischer, D. Miller, F. Tacchino, P. K. Barkoutsos, D. J. Egger, and I. Tavernelli, Ancilla-free implementation of generalized measurements for qubits embedded in a qudit space, arXiv:2203.07369.

[41] R. Majumdar, D. Madan, D. Bhoumik, D. Vinayagamurthy, S. Raghunathan, and S. Sur-Kolay, Optimizing ansatz design in QAOA for max-cut, arXiv:2106.02812.

[42] N. J. Cerf, M. Bourennane, A. Karlsson, and N. Gisin, Security of Quantum Key Distribution using *d*-Level Systems, Phys. Rev. Lett. **88**, 127902 (2002).

[43] Y.-H. Luo, H.-S. Zhong, M. Erhard, X.-L. Wang, L.-C. Peng, M. Krenn, X. Jiang, L. Li, N.-L. Liu, C.-Y. Lu, A. Zeilinger, and J.-W. Pan, Quantum Teleportation in High Dimensions, Phys. Rev. Lett. **123**, 070505 (2019).

[44] X.-M. Hu, C. Zhang, B.-H. Liu, Y. Cai, X.-J. Ye, Y. Guo, W.-B. Xing, C.-X. Huang, Y.-F. Huang, C.-F. Li, and G.-C. Guo, Experimental High-Dimensional Quantum Teleportation, Phys. Rev. Lett. **125**, 230501 (2020).

[45] E. Bisong, *Google Colaboratory* (Apress, Berkeley, CA, 2019), pp. 59–64.

[46] https://github.com/amitsaha2806/Moving.